A Journal of the Gesellschaft Deutscher Chemiker

Angewandte International Edition Chemie

GDCh

www.angewandte.org

Accepted Article

Title: Synthesis of Triply Fused Porphyrin-Nanographene Conjugates

Authors: Qiang Chen, Luigi Brambilla, Lakshya Daukiya, Kunal S. Mali, Steven De Feyter, Matteo Tommasini, Klaus Müllen, and Akimitsu Narita

To be cited as: *Angew. Chem. Int. Ed.* 10.1002/anie.201805063
Angew. Chem. 10.1002/ange.201805063

Link to VoR: http://dx.doi.org/10.1002/anie.201805063
http://dx.doi.org/10.1002/ange.201805063

WILEY-VCH

10.1002/anie.201805063

WILEY-VCH

Synthesis of Triply Fused Porphyrin-Nanographene Conjugates

Qiang Chen, Luigi Brambilla, Lakshya Daukiya, Kunal S. Mali, Steven De Feyter, Matteo Tommasini, Klaus Müllen,* and Akimitsu Narita*

Abstract: Two unprecedented porphyrin fused nanographene molecules **1** and **2** have been synthesized by Scholl reaction of tailor-made precursors based on benzo[*m*]tetraphene-substituted porphyrins. The chemical structures were validated by a combination of high-resolution matrix-assisted laser desorption/ionization time-of-flight mass spectrometry (HR MALDI-TOF MS), IR and Raman spectroscopy, and scanning tunnelling microscopy (STM). The UV-vis-near infrared absorption spectroscopy of **1** and **2** demonstrated broad and largely red-shifted absorption spectra extending up to 1000 and 1400 nm, respectively, marking the significant extension of the p-conjugated systems.

In the past decades, synthesis of p-extended porphyrins has attracted immense interests for their unique optical and electronic properties,[1] which render them highly valuable for a variety of applications, e.g., as near-infrared (NIR) dyes,[2] organic semiconductors,[3] and nonlinear optical materials.[4] Various aromatic hydrocarbons, including benzene,[5] naphthalene,[1c, 6] pyrene,[7] azulene,[8] corannulene[9] and coronene,[10] have thus been fused to the *meso*- and b-positions of porphyrin. More recently, Anderson and his colleagues have explored the p-extension of porphyrin with anthracene subunits, which have the geometry that fully matches the periphery of porphyrin and can form three C-C bonds (Scheme 1a).[11] Mono-, bis-, and tetrakis-anthracene-fused porphyrins have thus been reported, demonstrating markedly red-shifted UV-vis-near infrared (NIR) absorption spectra and reduced highest occupied molecular orbitalï lowest unoccupied molecular orbital (HOMO-LUMO) gaps. However, further p-extension of porphyrin cores by fusion with larger polycyclic aromatic hydrocarbons (PAHs) has remained challenging.

Large PAHs, which can be regarded as nanographenes,[12] are known to exhibit attractive (opto)electronic properties and self-assembly behavior,[13] which can be further fine-tuned by precise control over their size, shape, and edge structure.[14] Hexa-*peri*-hexabenzocoronene (HBC) with 42 sp^2-hybridized carbons has been extensively investigated as an archetypal nanographene.[15] Recently, we have achieved a synthesis of p-extended HBC with four extra K-regions, namely ñisolatedò double bonds that do not belong to the Clar sextets, employing a precursor having benzo[*m*]tetraphene units.[16] The K-regions shaped zigzag edges at the HBC periphery, which significantly lowered the HOMOï LUMO gap.

In recent years, numerous efforts have been made to introduce nanographenes as substituents to the periphery of porphyrin for making hybrid structures with tunable photophysical characteristics. For example, covalently bonded HBC-porphyrin conjugates have been synthesized, showing efficient energy transfer from HBC substituents to the porphyrin unit (Scheme 1b).[17] More recently, porphyrin was successfully bonded to two graphene nanoribbons.[18] However, the nanographene substituents can rotate with respect to the porphyrin core in such systems, which limits intramolecular conjugation. Moreover, the previous structural designs do not allow planarization of the porphyrin and nanographene units through formation of additional sextet rings. Here, we report a synthesis of b-,*meso*-,b-triply fused porphyrin-nanographene conjugates **1** and **2** by fusing porphyrin with p-extended HBCs with two extra K-regions. The zigzag edge of an anthracene substructure shaped at the periphery of HBC can geometrically fit *meso*- and b-positions of porphyrin (Scheme 1c). The fully conjugated planar structures facilitate electron delocalization over the porphyrin and HBC units, which induced narrowing of the HOMO-LUMO gap and large red-shifts in the UV-vis-NIR absorption spectra. STM measurements also validated the planar structure of **2** while showing its bilayer assembly behavior at the interface of 1,2,4-trichlorobenzene (TCB) and highly oriented pyrolytic graphite (HOPG).

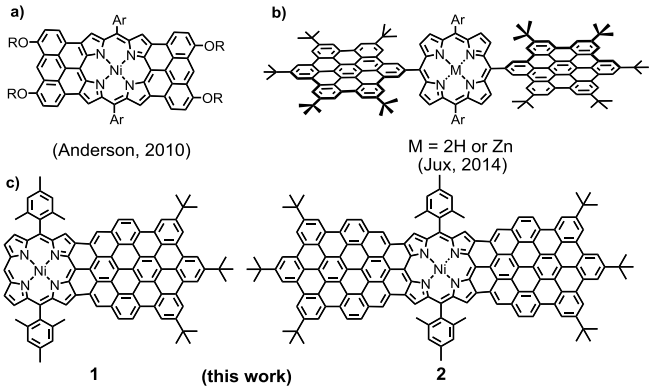

Scheme 1. Structures of (a) bis-anthracene fused porphyrin; (b) covalently connected HBC-porphyrin conjugates, and (c) triply fused porphyrin-nanographene conjugates **1** and **2**.

As shown in Scheme 3, the synthesis of targeted porphyrin-nanographene conjugates **1** and **2** was carried out

[*] Q. Chen, Prof. Dr. K. Müllen, Dr. A. Narita
Max Planck Institute for Polymer Research
Ackermannweg 10, 55128 Mainz (Germany)
E-mail: muellen@mpip-mainz.mpg.de
narita@mpip-mainz.mpg.de
Dr. L. Brambilla, Prof. M. Tommasini
Dipartimento di Chimica, Materiali ed Ingegneria Chimica ñG. Nattaò
Politecnico di Milano
Piazza Leonardo da Vinci, 32, 20133 Milano (Italy)
Dr. L. Daukiya, Dr. K. S. Mali, Prof. Dr. S. De Feyter
KU Leuven, Department of Chemistry
Division of Molecular Imaging and Photonics
Celestijnenlaan 200F, B-3001 Leuven (Belgium)

Supporting information for this article is given via a link at the end of the document.

10.1002/anie.201805063

through cyclodehydrogenation of corresponding precursors **19** and **20**, respectively, which were based on benzo[*m*]tetraphene-substituted porphyrins. Precursors **19** and **20** were obtained by Suzuki coupling of boronate ester **17** and dibromoporphyrin (Ni) **18**. The key intermediate **17** was synthesized as displayed in Scheme 2. First, triisopropylsilyl (TIPS)-ethynylbiphenylboronic acid **10** was prepared from 1-bromo-3-*tert*-butylbenzene (**3**). Lithium halogen exchange of **3** using *n*-BuLi at ï 78 ęC followed by quenching with triisopropylborate and hydrolysis gave (3-*tert*-butylphenyl)boronic acid (**4**) in 66% yield. Suzuki coupling of **4** with 4-bromo-2-nitroaniline provided 3-nitro-4-aminobiphenyl **5** in 88% yield, which was subjected to Sandmeyer iodination to afford 4-iodo-3-nitrobiphenyl **6** in 85% yield. Reduction of **6** produced 3-amino-4-iodobiphenyl **7** in 98% yield, which was subjected to Sonogashira coupling with TIPS-acetylene to provide 3-amino-4-TIPS-ethynylbiphenyl **8** in 99% yield. Finally, Sandmeyer iodination gave 3-iodo-4-TIPS-ethynylbiphenyl **9** in 88% yield, which was treated with *n*-BuLi and quenched with triisopropylborate ester followed by hydrolysis to obtain desired boronic acid **10** in 86% yield.

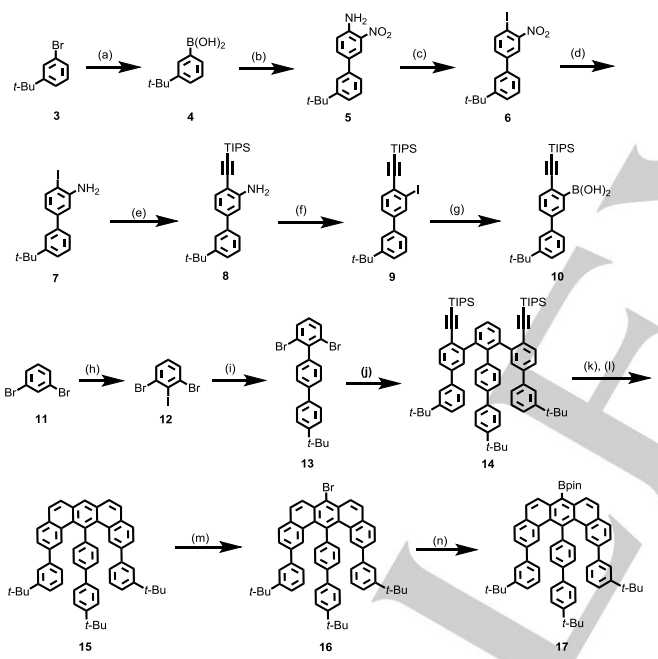

Scheme 2. Synthesis of boronate ester **17**. Reagents and conditions: a) (1) *n*-BuLi, ş78 ÁC, 3 h, (2) B(*i*-PrO)$_3$, ş78 ÁC to r.t., 17 h, (3) 1 N HCl, r.t., 0.5 h, 66%; b) 4-bromo-2-nitroaniline, Pd(PPh$_3$)$_4$, Na$_2$CO$_3$, toluene/EtOH/H$_2$O = 3:1:1, 100 °C, 24 h, 88%; c) (1) PTSAĂH$_2$O, NaNO$_2$, acetonitrile/H$_2$O = 10:1, 0 °C, 2 h, (2) KI, 0 °C to r.t., overnight, 85%; d) Fe powder, AcOH/EtOH = 1:1, reflux, 1 h, 98%; e) TIPS-acetylene, Pd(PPh$_3$)$_2$Cl$_2$ĂCH$_2$Cl$_2$, CuI, THF:TEA = 2:1, r.t., 5 h, 99%; f) (1) PTSAĂH$_2$O, NaNO$_2$, KI, acetonitrile/H$_2$O = 10:1, 0 °C to r.t., 21 h, 88%; g) (1) *n*-BuLi, THF, ş78 ÁC, 0.5 h, (2) B(*i*-PrO)$_3$, ş78 ÁC for 0.5 h then r.t. for 1 h, (3) 1 N HCl, r.t., 0.5 h, 86%; h) LDA, ş78 ÁC, 2 h, then I$_2$, ş78 ÁC, 2 h, 76%; i) (4'-(*tert*-butyl)-[1,1'-biphenyl]-4-yl)boronic acid, Pd(PPh$_3$)$_4$, Na$_2$CO$_3$, toluene/EtOH/H$_2$O = 3:1:1, 100 °C, 48 h, 70%; j) **10**, Pd(PPh$_3$)$_4$, K$_2$CO$_3$, 1,4-dioxane/H$_2$O = 3:1, 100 °C, 14 h, 86%; k) TBAF, THF, r.t., 2 h, 100%; l) PtCl$_2$, toluene, 80 °C, 24 h, 65%; m) Br$_2$, CH$_2$Cl$_2$, r.t., 1 h, 91%; n) AcOK, Pd(dppf)Cl$_2$ĂCH$_2$Cl$_2$, DMF, 80ÁC, 24 h, 83%. PTSA ş *p*-toluenesulfonic acid, TIPS ş triisopropylsilyl, THF ï tetrahydrofuran, TEA ş trimethylamine, LDA ş lithium diisopropylamide, TBAF ş tetrabutylammonium fluoride, DMF ï dimethylformamide.

On the other hand, for the preparation of 2,6-dibromoterphenyl **13**, 1,3-dibromobenzene (**11**) was first subjected to selective lithiation by lithium diisopropylamide (LDA) and subsequently treated with I$_2$ to give 1,3-dibromo-2-iodobenzene (**12**) in 76% yield. Selective Suzuki coupling of **12** with (4'-(*tert*-butyl)-[1,1'-biphenyl]-4-yl)boronic acid provided **13** in 70% yield. Then, Suzuki coupling of **13** and 2.0 equivalents of **10** afforded bis(TIPS-ethynyl)quinquephenyl **14** in 86% yield. After deprotection and Pt-catalyzed cycloaromatization, benzo[*m*]tetraphene **15** was obtained in 65% yield. The *meso*-position of **15** could be selectively brominated to provide 7-bromo-benzo[*m*]tetraphene **16** in 91% yield, which was converted to boronate ester **17** by Miyaura borylation in 83% yield. The structure of **17** was characterized by using ^{1}H NMR, ^{13}C NMR, and high-resolution mass spectrometry (see Figures S45 and S46).

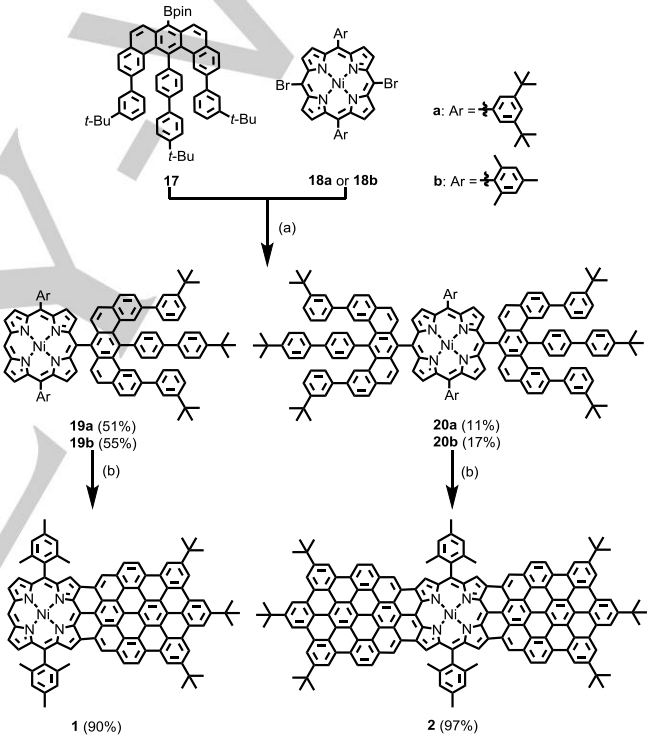

Scheme 3. Syntheses of triply fused porphyrin-nanographene conjugates **1** and **2**. Reagents and conditions: a) (1) Pd(PPh$_3$)$_4$, K$_2$CO$_3$, toluene/DMF = 1:1, 110 °C, 36 h, then (2) Pd(PPh$_3$)$_4$, triethylamine, formic acid, toluene, 100 °C, 2 h; b) DDQ, CH$_2$Cl$_2$/triflic acid = 100:1, r.t., 10 h, Ar = mesityl.

For the synthesis of precursors **19** and **20**, two dibromo-substituted porphyrin (Ni) derivatives **18a**[19] and **18b**[20] with bulky substituents were selected to increase the solubility of the final products in common organic solvents,[19, 21] and prepared following reported methods (see synthetic details in Supporting Information). The nickel (II) ion was inserted into the porphyrin core considering the high stability of nickel (II)-porphyrin under strong oxidation conditions required for the final Scholl reaction.[11c] The Suzuki coupling of boronate ester **17** and dibromoporphyrin **18a**/**b** provided corresponding one- and two-

fold coupling products **19a**, **20a**, **19b**, and **20b** in 51%, 11%, 55%, and 17% yield, respectively. The structures of these coupling products were unambiguously characterized by ^{1}H NMR, ^{13}C NMR, and high-resolution matrix-assisted laser desorption/ionization time-of-flight mass spectrometry (HR MALDI-TOF MS). All the proton signals could be assigned with the help of ^{1}H,^{1}H-correlation spectroscopy (COSY), ^{1}H,^{1}H-nuclear overhauser enhancement spectroscopy (NOESY), and ^{1}H,^{1}H-total correlation spectroscopy (TOCSY) spectra (see Figures 1a and S1). Although growing single crystals of **19** suitable for X-ray diffraction analysis failed under various conditions, we successfully obtained a single crystal of **20b** by slow evaporation of its dichloromethane solution at room temperature, allowing the unambiguous structural confirmation by single-crystal X-ray analysis (Figure 1b).

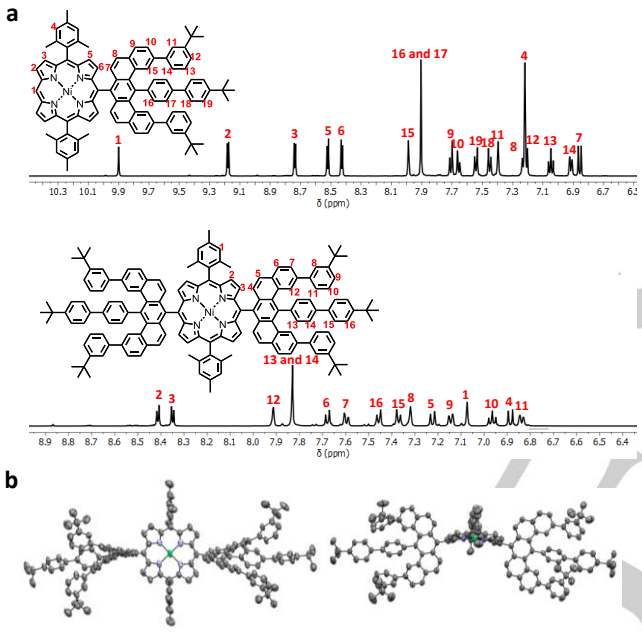

Figure 1. a) Aromatic region of the ^{1}H NMR spectra of **19b** (top) and **20b** (bottom) measured in CD_2Cl_2 at 298 K (500 MHz); b) X-ray crystallographic structure of **20b** (measured at 193 K): top view (left) and front view (right). Atom colors: C-gray; N-blue; Ni-green. Hydrogen atoms and solvents have been omitted for clarity.

The Scholl reaction of **19a** was first attempted with $FeCl_3$, which is widely used for cyclodehydrogenation of polyphenylenes and also employed in previous syntheses of p-extended porphyrin derivatives.[11b, 11c] However, MALDI-TOF MS analysis of the reaction mixture indicated the presence of partially fused species even after the reaction overnight in addition to significant chlorination (see Figure S2). On the other hand, use of 2,3-dichloro-5,6-dicyano-1,4-benzoquinone (DDQ) with catalytic amount of triflic acid turned out to be effective, providing completely dehydrogenated product (formation of 8 carbon-carbon bonds) together with over-dehydrogenated byproducts (formation of 10 carbon-carbon bonds). We assumed that the over-dehydrogenation was caused by the formation of five-membered rings between the 3,5-di-*tert*-butylphenyl groups and the porphyrin core (see Figure S3), similar to observations in a previous report on electron deficient porphyrin (Ni) systems.[22] To avoid this undesired side reaction, we next employed precursors **19b** and **20b** with mesityl groups. To our delight, the oxidative cyclodehydrogenation of **19b** and **20b** with DDQ and a catalytic amount (100:1, v/v) of triflic acid successfully provided triply fused porphyrin-nanographene conjugates **1** and **2**, respectively, in 90% and 97% yields.

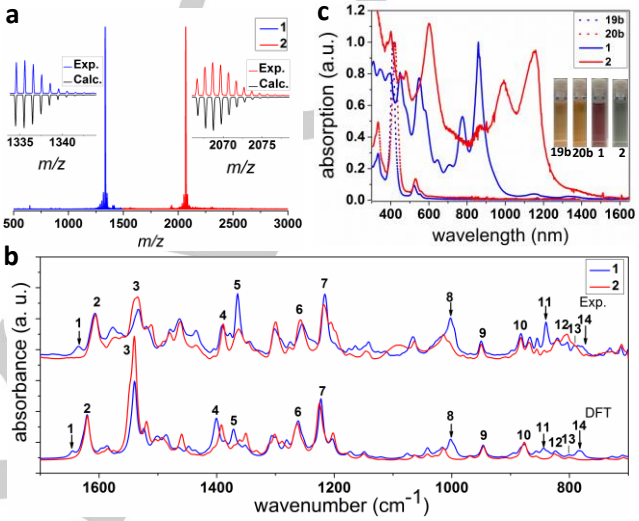

Figure 2. a) MALDI-TOF MS spectra of porphyrin-nanographene conjugates **1** and **2**, inset: experimental and theoretical isotopic distribution patterns; b) Experimental FT-IR spectra of **1** and **2** compared with simulated spectra obtained from DFT calculations (computed wavenumbers have been scaled by 0.98). Characteristic features of **1** are marked with arrows (see Table S1 and Figure S5 for details); c) UV-vis-NIR absorption spectra of **1** and **2** in comparison with corresponding precursors **19b** and **20b** measured in tetrahydrofuran at room temperature. The inset photographs show the tetrahydrofuran solutions of **19b**, **20b**, **1**, and **2**.

The strong intermolecular interactions of both **1** and **2** prevented their characterization by NMR spectroscopy. High temperature ^{1}H NMR measurement at 140 °C in *o*-dichlorobenzene-d_4 and addition of CS_2 in an attempt to prevent the aggregation failed to give highly resolved spectra. The possibility of the presence of remaining radical cation species was excluded by addition of hydrazine as quencher. Attempts to remove the nickel (II) ion in **1** by treatment with trifluoroacetic acid and sulfuric acid resulted in its decomposition. Nevertheless, characterizations by high-resolution MALDI-TOF MS, IR and Raman spectroscopy, and STM clearly verified the formation of the desired structures. MALDI-TOF MS analysis demonstrated the removal of 16 and 32 protons for **19b** and **20b**, respectively, after cyclodehydrogenation reaction (see Figure S4), corroborating the complete dehydrogenation. High-resolution mass spectra of **1** and **2** display intense signals at *m/z* = 1334.4831 and 2066.7644, which are in good agreement with calculated molecular mass of 1334.4797 and 2066.7614, respectively. Furthermore, the observed isotopic distribution

patterns are fully consistent with the calculated spectra (Figure 2a).

Figure 2b shows the experimental FT-IR spectra of **1** and **2** compared with the simulated spectra obtained from density functional theory (DFT) calculations. The overall agreement between the experimentally measured and simulated spectra provides strong support for the successful synthesis of both compounds. Moreover, the observed differences between the IR spectra can be traced back to the distinct features in their chemical structures. For instance, both **1** and **2** display IR bands at 1606/1605, 1532/1534, 819/820, and 803 cm^{-1}, which can be attributed to vibration modes of chemical features common to both structures (Figure S5). In contrast, the IR bands located at 1634, 1001, 838, and 790 cm^{-1} are only observed for **1** (see arrows in Figure 2b), and indeed characteristic for the bare periphery of the porphyrin unit (see Table S1 and Figure S5 for the details about the assignment of the IR bands mentioned above). The FT-Raman spectra of **1** and **2** showed a fluorescence background, which hindered a precise analysis of the Raman features. However, good overal agreement between the experimentally obtained characteristic peaks and DFT results further corroborated the desired structures (see Figure S6 ǵ S8).

The optical properties of **1** and **2** were studied by UV-vis-NIR absorption spectrometry in tetrahydrofuran in comparison with corresponding precursors **19b** and **20b**, respectively (Figure 2c). Both precursors exhibited intense absorption peaks at 420 and 560 nm, which could be assigned to the Soret and Q band of the nickel (II) porphyrin core, respectively.[11b] After expansion of the p-systems by cyclodehydrogenation, the maximum absorption peak of **1** is red-shifted to 866 nm with the tail extended to around 1000 nm. Fusion of another nanographene unit to the porphyrin core red-shifted the maximum absorption peak of **2** to 1176 nm with the tail extending to approximately 1400 nm. The observed absorption bands were in good agreement with the simulation by time-dependent DFT (TDDFT) calculations (see Figure S11). The HOMO/LUMO energy levels of **1** and **2** were calculated by DFT to be ï 4.53 eV/ï 2.75 eV and ï 4.23 eV/ï 2.88 eV, respectively, corresponding to low HOMO-LUMO gaps of 1.78 eV and 1.35 eV. Fluorescence measurements on these molecules were not successful because of the heavy atom effect of the central Ni^{2+} ion, which quenched the luminescence.[23]

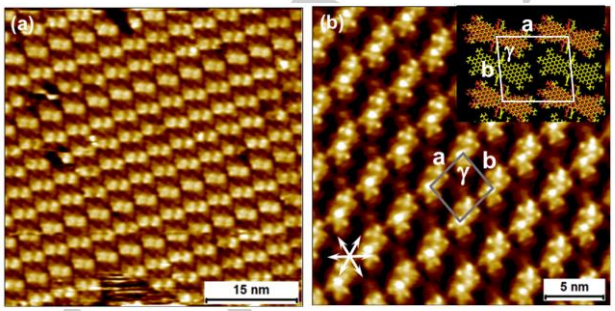

Figure 3. STM characterization of **2** at the TCB/HOPG interface. (a) Large-scale STM image showing long-range ordered assembly of **2**; (b) High-resolution STM image of the self-assembled network. Unit cell parameters: a = 3.7 ° 0.1 nm, b = 4.0 ° 0.1 nm and g = 86 ° 2¯. The graphite symmetry axes are shown in the lower left corner. The inset displays proposed molecular model for the bilayer self-assembly. The molecules in yellow form a continuous, densely packed lower layer whereas those in red occupy the second layer. Imaging parameters (a) V_{bias} = -1.1 V, I_{set} = 50 pA (b) V_{bias} = -900 mV, I_{set} = 85 pA.

STM analysis of **2** at the TCB/HOPG interface revealed a self-assembled network consisting of an ordered array of C_2-symmetric dumbbell-shaped features. The size and shape of these features agrees well with the expected shape and size of **2** (Figure 3a). At each end of these features, three lobes could be discerned, representing the peripheral *tert*-butyl groups (Figure 3b). The molecules were close-packed along one of the unit cell vectors (vector a), but well-separated from each other along the other (vector b) unit cell vector. Such packing is rather unusual, since a close-packed structure is expected considering the lack of specific functional groups on the periphery of this molecule. We ascribe this packing to formation of a bilayer film with a continuous first layer adsorbed on HOPG and a discontinuous second layer, presumably due to steric repulsion, as displayed in a proposed molecular model (Figure 3b, inset). Only the molecules in the second layer (in yellow color in Figure 3b, inset) were observed in STM images, as confirmed by investigating the edge of molecular domains (see more detailed discussion in the Supporting Information).

In conclusion, we have synthesized two triply fused porphyrin-nanographene conjugates **1** and **2** through the cyclodehydrogenation of carefully designed precursors featuring benzo[*m*]tetraphene-substituted porphyrins. The significantly p-extended porphyrins have small HOMO-LUMO gaps of 1.78 eV and 1.35 eV based on DFT calculations. The optical absorption spectra of **1** and **2** were considerably red-shifted to the NIR region, making them of high potential as NIR dyes for optoelectronic applications such as infrared sensing. This strategy for fusion of porphyrin cores into nanographene planes can potentially be applied to synthesize a large variety of hybrid structures, for example porphyrin-fused graphene nanoribbons (GNRs). Further synthetic studies on these extended structures are ongoing in our group.

Acknowledgements

We are grateful for the financial support from the Max Planck Society and EC through the Graphene Flagship and Marie-Curie ITN project ñSwitchò(GA No. 642196). This work was supported in part by FWO under EOS 30489208, and internal funds ï KU Leuven.

Keywords: nanographene Å porphyrin Å Scholl reaction Å p-extension Ånear-infrared absorption

Reference

[1] a) M. Stepien, E. Gonka, M. Zyla, N. Sprutta, *Chem. Rev.* **2017**, *117*, 3479-3716; b) T. D. Lash, T. M. Werner, M. L. Thompson, J. M. Manley, *J. Org. Chem.* **2001**, *66*, 3152-3159; c) H. S. Gill, M. Harmjanz, J. Santamaria, I. Finger, M. J. Scott, *Angew. Chem. Int. Ed.* **2004**, *43*, 485-490; d) Y. Nakamura, N. Aratani, H. Shinokubo, A. Takagi, T. Kawai, T. Matsumoto, Z. S. Yoon, D. Y. Kim, T. K. Ahn, D. Kim, A. Muranaka, N. Kobayashi, A. Osuka, *J. Am. Chem. Soc.* **2006**, *128*,

4119-4127; e) S. Hiroto, Y. Miyake, H. Shinokubo, *Chem. Rev.* **2017**, *117*, 2910-3043; f) T. Tanaka, A. Osuka, *Chem. Soc. Rev.* **2015**, *44*, 943-969; g) H. Mori, T. Tanaka, A. Osuka, *J. Mater. Chem. C* **2013**, *1*, 2500; h) A. Osuka, T. Tanaka, *Chem. Eur. J.* **2018** (in press), doi: 10.1002/chem.201802810.

[2] C. Jiao, N. Zu, K. W. Huang, P. Wang, J. Wu, *Org. Lett.* **2011**, *13*, 3652-3655.

[3] M. H. Sayyad, M. Saleem, K. S. Karimov, M. Yaseen, M. Ali, K. Y. Cheong, A. F. Mohd Noor, *Appl. Phys. A* **2009**, *98*, 103-109.

[4] N. Aratani, D. Kim, A. Osuka, *Chem. Asian J.* **2009**, *4*, 1172-1182.

[5] a) L. Barloy, D. Dolphin, D. Dupre, T. P. Wijesekera, *J. Org. Chem.* **1994**, *59*, 7976-7985; b) S. Richeter, C. Jeandon, J.-P. Gisselbrecht, R. Ruppert, H. J. Callot, *J. Am. Chem. Soc.* **2002**, *124*, 6168-6179; c) S. Fox, R. W. Boyle, *Chem. Commun.* **2004**, 1322-1323; d) D. M. Shen, C. Liu, Q. Y. Chen, *Chem Commun (Camb)* **2005**, 4982-4984; e) D. M. Shen, C. Liu, Q. Y. Chen, *J. Org. Chem.* **2006**, *71*, 6508-6511.

[6] a) A. N. Cammidge, P. J. Scaife, G. Berber, D. L. Hughes, *Org. Lett.* **2005**, *7*, 3413-3416; b) M. Tanaka, S. Hayashi, S. Eu, T. Umeyama, Y. Matano, H. Imahori, *Chem. Commun.* **2007**, 2069-2071.

[7] a) O. Yamane, K.-i. Sugiura, H. Miyasaka, K. Nakamura, T. Fujimoto, K. Nakamura, T. Kaneda, Y. Sakata, M. Yamashita, *Chem. Lett.* **2004**, *33*, 40-41; b) V. V. Diev, K. Hanson, J. D. Zimmerman, S. R. Forrest, M. E. Thompson, *Angew. Chem. Int. Ed.* **2010**, *49*, 5523-5526.

[8] K. Kurotobi, K. S. Kim, S. B. Noh, D. Kim, A. Osuka, *Angew. Chem. Int. Ed.* **2006**, *45*, 3944-3947.

[9] K. Ota, T. Tanaka, A. Osuka, *Org. Lett.* **2014**, *16*, 2974-2977.

[10] V. V. Diev, C. W. Schlenker, K. Hanson, Q. Zhong, J. D. Zimmerman, S. R. Forrest, M. E. Thompson, *J. Org. Chem.* **2012**, *77*, 143-159.

[11] a) N. K. Davis, M. Pawlicki, H. L. Anderson, *Org. Lett.* **2008**, *10*, 3945-3947; b) N. K. Davis, A. L. Thompson, H. L. Anderson, *Org. Lett.* **2010**, *12*, 2124-2127; c) N. K. Davis, A. L. Thompson, H. L. Anderson, *J. Am. Chem. Soc.* **2011**, *133*, 30-31.

[12] L. Chen, Y. Hernandez, X. Feng, K. Mullen, *Angew. Chem. Int. Ed.* **2012**, *51*, 7640-7654.

[13] a) J. Wu, A. Fechtenkotter, J. Gauss, M. D. Watson, M. Kastler, C. Fechtenkotter, M. Wagner, K. Mullen, *J. Am. Chem. Soc.* **2004**, *126*, 11311-11321; b) L. F. Dossel, V. Kamm, I. A. Howard, F. Laquai, W. Pisula, X. Feng, C. Li, M. Takase, T. Kudernac, S. De Feyter, K. Mullen, *J. Am. Chem. Soc.* **2012**, *134*, 5876-5886; c) X. Feng, W. Pisula, T. Kudernac, D. Wu, L. Zhi, S. De Feyter, K. Mullen, *J. Am. Chem. Soc.* **2009**, *131*, 4439-4448; d) Y. Yamamoto, T. Fukushima, Y. Suna, N. Ishii, A. Saeki, S. Seki, S. Tagawa, M. Taniguchi, T. Kawai, T. Aida, *Science* **2006**, *314*, 1761-1764.

[14] S. Fujii, T. Enoki, *Accounts. Chem. Res.* **2012**, *46*, 2202-2210.

[15] J. Holzwarth, K. Y. Amsharov, D. I. Sharapa, D. Reger, K. Roshchyna, D. Lungerich, N. Jux, F. Hauke, T. Clark, A. Hirsch, *Angew. Chem. Int. Ed.* **2017**, *56*, 12184-12190.

[16] T. Dumslaff, B. Yang, A. Maghsoumi, G. Velpula, K. S. Mali, C. Castiglioni, S. De Feyter, M. Tommasini, A. Narita, X. Feng, K. Mullen, *J. Am. Chem. Soc.* **2016**, *138*, 4726-4729.

[17] a) J. M. Englert, J. Malig, V. A. Zamolo, A. Hirsch, N. Jux, *Chem. Commun.* **2013**, *49*, 4827-4829; b) D. Lungerich, J. F. Hitzenberger, M. Marcia, F. Hampel, T. Drewello, N. Jux, *Angew. Chem. Int. Ed.* **2014**, *53*, 12231-12235.

[18] W. Perkins, F. R. Fischer, *Chem. Eur. J.* **2017**, *23*, 17687-17691.

[19] O. B. Locos, D. P. Arnold, *Org. Biomol. Chem.* **2006**, *4*, 902-916.

[20] L. Yu, K. Muthukumaran, I. V. Sazanovich, C. Kirmaier, E. Hindin, J. R. Diers, P. D. Boyle, D. F. Bocian, D. Holten, J. S. Lindsey, *Inorg. Chem.* **2003**, *42*, 6629-6647.

[21] K. Jyothish, Q. Wang, W. Zhang, *Adv. Synth. Catal.* **2012**, *354*, 2073-2078.

[22] N. Fukui, S.-K. Lee, K. Kato, D. Shimizu, T. Tanaka, S. Lee, H. Yorimitsu, D. Kim, A. Osuka, *Chem. Sci.* **2016**, *7*, 4059-4066.

[23] A. Harriman, *J. Chem. Soc., Faraday Trans. 1* **1980**, *76*, 1978.

10.1002/anie.201805063

WILEY-VCH

Entry for the Table of Contents (Please choose one layout)

Layout 1:

COMMUNICATION

Triply fused porphyrin-nanographene conjugates have been synthesized by Scholl reaction of tailor-made porphyrin based precursors, showing broad and intense near infrared absorption. Self-assembled bilayer of **2** was observed at the trichlorobenzene/highly oriented pyrolytic graphite (HOPG) interface.

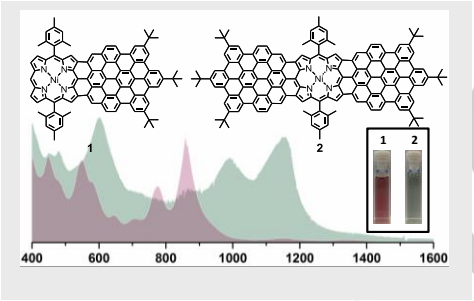

Qiang Chen, Luigi Brambilla, Lakshya Daukiya, Kunal S. Mali, Steven De Feyter, Matteo Tommasini, Klaus Müllen, and Akimitsu Narita**

Page 1. – Page 5.

Synthesis of Triply Fused Porphyrin Nanographene Conjugates

Layout 2:

COMMUNICATION

((Insert TOC Graphic here))

Text for Table of Contents

*Author(s), Corresponding Author(s)**

Page No. – Page No.

Title